CARBON 50 (2012) 4953–4964

Available at www.sciencedirect.com

SciVerse ScienceDirect

journal homepage: www.elsevier.com/locate/carbon

Metal-assisted hydrogen storage on Pt-decorated single-walled carbon nanohorns

Yun Liu [a,b,*], Craig M. Brown [a], Dan A. Neumann [a], David B. Geohegan [c], Alexander A. Puretzky [c], Christopher M. Rouleau [c], Hui Hu [d], David Styers-Barnett [e], Pavel O. Krasnov [f,h], Boris I. Yakobson [f,g]

[a] National Institute of Standards and Technology, Center for Neutron Research, Gaithersburg, MD 20899, USA
[b] Department of Chemical Engineering, University of Delaware, Newark, DE 19716, USA
[c] Oak Ridge National Laboratory, Oak Ridge, TN 37831-6056, USA
[d] Chase Corporation, 295 University Ave., Westwood, MA 02090, USA
[e] Department of Chemistry, University of Indianapolis, 1400 East Hanna Ave., Indianapolis, IN 46227, USA
[f] Department of Materials Science and Mechanical Engineering and Department of Chemistry, Rice University, Houston, TX 77005, USA
[g] Department of Chemistry, Rice University, Houston, TX 77005, USA
[h] Department of Physics, Siberian State Technological University, 660049, Russia

ARTICLE INFO

Article history:
Received 18 August 2011
Accepted 18 June 2012
Available online 23 June 2012

ABSTRACT

The catalytic dissociation of hydrogen molecules by metal nanoparticles and spillover of atomic hydrogen onto various supports is a well-established phenomenon in catalysis. However, the mechanisms by which metal catalyst nanoparticles can assist in enhanced hydrogen storage on high-surface area supports are still under debate. Experimental measurements of metal-assisted hydrogen storage have been hampered by inaccurate estimation of atomically stored hydrogen deduced from comparative measurements between metal-decorated and undecorated samples. Here we report a temperature cycling technique combined with inelastic neutron scattering (INS) measurements of quantum rotational transitions of molecular H_2 to more accurately quantify adsorbed hydrogen aided by catalytic particles using single samples. Temperature cycling measurements on single-wall carbon nanohorns (SWCNHs) decorated with 2–3 nm Pt nanoparticles showed 0.17% mass fraction of metal-assisted hydrogen storage (at ≈0.5 MPa) at room temperature. Temperature cycling of Pt-decorated SWCNHs using a Sievert's apparatus also indicated metal-assisted hydrogen adsorption of ≈0.08% mass fraction at 5 MPa at room temperature. No additional metal-assisted hydrogen storage was observed in SWCNH samples without Pt nanoparticles cycled to room temperature. The possible formation of C–H bonds due to spilled-over atomic hydrogen was also investigated using both INS and density functional theory calculations.

1. Introduction

Increasing concerns over future energy resources, global production of carbon dioxide and impacts of global warming are driving society to search for a replacement for fossil fuels and to improve clean energy technologies. Among the new avenues being pursued, hydrogen is seen as a clean energy carrier for transportation. However, one major obstacle for

* *Corresponding author at:* NIST Center for Neutron Research, 100 Bureau Drive MS6102, Gaithersburg, MD 20899, USA. Fax: +1 301 9219847.
E-mail address: yun.liu@nist.gov (Y. Liu).
0008-6223/$ - see front matter
http://dx.doi.org/10.1016/j.carbon.2012.06.028

moving to a future hydrogen economy is the lack of suitable on-board hydrogen storage media, which urgently requires a technology breakthrough [1].

In recent years, Yang and co-workers have reported that the catalytic dissociation of hydrogen on metals and subsequent spillover onto various supports can greatly increase hydrogen storage at ambient temperature [2–5]. This metal-assisted hydrogen adsorption was reversible with applied pressure at ambient temperature [2–4,6,7]. Systems based on Pt-decorated metal organic frameworks (MOFs) were reported to achieve ≈4% mass fraction excess hydrogen storage at 10 MPa gas pressure and room temperature [3]. And Pt-doped activated carbon samples achieved ≈1.2% mass fraction under the same conditions [5]. Since high surface-area carbon samples typically only store up to ≈0.6% mass fraction or less by physisorption at room temperature and 10 MPa [5,6,8–11] due to the small hydrogen adsorption enthalpy [12,13], the additional hydrogen storage in these metal-decorated samples at room temperature has been associated with the hydrogen spillover effect that has been well investigated in catalysis [3,4].

Several groups have attempted to repeat these early experiments. However they did not observe such large enhancements [9,11]. Reasons given for this irreproducibility include considerations that the hydrogen adsorption capacity of a sample can be very sensitive to subtle changes in experimental conditions including the control of metal particle size, the sample pretreatment temperature, and the dead volume of a Sievert's apparatus [14,15]. Further complications have arisen as some experimental evidence suggests that other elements/molecules such as oxygen and water molecules on a carbon surface may play important roles [16–19].

Thus, while spillover is a well investigated and extensively reviewed topic in catalysis [20–24], and an essential process by which metals can enhance hydrogen storage at ambient temperatures, it appears likely that it may be just one of several factors that determine the overall efficacy. The fate of the hydrogen atoms on the support surface, including rates for adsorption, diffusion, recombination and desorption as hydrogen molecules, are also important. Therefore, the combined physical and chemical mechanisms by which metal particles assist in the hydrogen storage in metal-decorated samples will thus be more generally referred to as "metal-assisted hydrogen storage".

In fact, there is no quantitative direct measurement of the amount of metal-assisted hydrogen adsorption in the presence of large amount of physisorbed hydrogen molecules despite the plethora of experimental reports as traditional methods can either overestimate or underestimate the metal-assisted hydrogen storage. Typically, experiments in the hydrogen storage community that are used to estimate the amount of metal-assisted hydrogen adsorption involve measurements on two separate samples [3,4,9,11,16,18,25,26]. One sample is treated to enhance the spillover process; the other is a reference sample which can be a precursor material without catalytic particles or a physical mixture of different materials without special treatment. By comparing hydrogen adsorption isotherms from the two samples, any increase of the hydrogen storage in the metal doped sample is then attributed to the metal-assisted adsorption. Because the physisorption capacity can be dramatically different in the two samples, the enhancement in adsorption may significantly overestimate or underestimate the extra hydrogen adsorption due to the presence of catalytic metal particles.

In this paper, we report two methods that provide quantitative and accurate measurement of the amount of temperature-activated hydrogen adsorption induced by metal decoration. Inelastic neutron scattering (INS) and high pressure gas sorption methods are described that both utilize a carefully designed temperature cycle to measure the amount of metal-assisted hydrogen adsorption in our SWCNH samples. The temperature cycling technique is tailored to investigate samples which involve thermally-activated catalytic processes (such as spillover) and therefore, unlike conventional methods, can quantify the amount of metal-assisted hydrogen storage in a single, metal-decorated sample without the need for comparison to a reference sample.

Our measurements indicate that there is indeed a measurable amount of metal-assisted hydrogen adsorption induced at room temperature in our Pt-SWCNH samples that remains observable at 77 K. The effect of the temperature and gas pressure on the adsorbed hydrogen in the presence of Pt clusters is also investigated. The INS method first proposed by us and described herein has been recently applied to measure hydrogen adsorption due to the spillover effect at room temperature in Pt-decorated activated carbon samples [27]. The details of this INS method and its limitations are presented in this paper for the first time.

2. Experimental

2.1. *Sample preparation*

Single wall carbon nanohorns were synthesized using high power laser vaporization [28,29]. A quartz tube (7.6 cm diameter, 122 cm length) is mounted inside a hinged tube furnace operating up to 1150 °C. The ends of the quartz tube were O-ring sealed with vacuum flanges and the entire system evacuated by a mechanical pump to control the growth environment. Argon is introduced around the laser entrance window to maintain specified pressures and flow rates to carry SWCNHs out of the furnace into a collection chamber fitted with a HEPA filter. The Nd:YAG (wavelength $\lambda = 1.064$ μm) laser light is delivered through a 0.6 mm diameter fiber optic cable and focused through an anti-reflection coated window onto a target positioned in the center of furnace. SWCNHs are synthesized at the optimized laser parameters using 20 ms laser pulses, ≈90 J/pulse at low laser pulse repetition rate of 5 Hz. The collimating ($f = 20$ cm) and focusing ($f = 1$ m) lenses mounted on a robotic arm can be moved to scan the laser beam (4 mm spot diameter) across the target in pre-designed raster patterns to achieve uniform target erosion during long time synthesis scans. Using this approach we are able to produce relatively large amounts of SWCNHs with high production rates of 10 g/h. SWCNHs were characterized using scanning and transmission electron microscopy (SEM and TEM), thermo-gravimetric analysis (TGA), and Raman scattering [28,29].

The as prepared nanohorns (AP-SWCNHs) (≈300 mg) were opened by oxidation in air, loaded in a quartz boat, and placed in a quartz tube. The sample was heated in a three-zone

furnace to 550 °C under flowing air and kept at this temperature for 20 min. After this the sample was cooled down to the room temperature. Decoration of opened nanohorns (O-SWCNH) with Pt was performed using a wet chemistry approach. In this case ≈100 mg of O-SWCNHs were mixed with 3 mL of 8% mass fraction H_2PtCl_6 and 340 mL of deionized H_2O and the mixture was sonicated for 2 h. After that ≈60 mL of 1% mass fraction of sodium citrate solution was added to the mixture and stirred at 80 °C for 4 h. After cooling to the room temperature, the mixture was filtered through a 1.0 μm pore-size filter membrane, and the solid residual was collected on the membrane and was dried at room temperature overnight. The weight of the final product was ≈130 mg. The Pt concentration is measured at around 20% mass fraction using the prompt-gamma activation analysis facility at the National Institute of Standards and Technology Center for Neutron Research (NCNR). The surface area of this Pt decorated opened SWCNH (Pt-SWCNH) is measured to be about 998 m^2/g. Prior to INS and high-pressure experiments, the SWCNH sample was heated to 200 °C under dynamic vacuum for about 15 h. The final residual pressure was better than 3×10^{-5} mbar.

2.2. Inelastic neutron scattering (INS)

INS spectra were collected using the Filter Analyzer Neutron Spectrometer (FANS) at the NCNR [30,31]. A pyrolytic graphite (0 0 2) monochromator was bracketed between two Söller collimators for measurements over the energy range ≈5–45 meV, while a Cu(2 2 0) monochromator was used for the energy range from ≈50 to ≈130 meV. The sample (734 mg of degassed Pt-SWCNH) was transferred to a cylindrical aluminum cell inside a glove box. The sample cell was mounted onto a sample stick and was carefully leak checked using a mass-spectrum based leak detector and subsequently evacuated to high vacuum using a turbomolecular pump. The sample stick was mounted into a temperature controlled top-loading closed-cycle refrigerator with helium exchange gas around the sample can. An equivalent amount of hydrogen corresponding to 1% mass fraction loading was admitted to the sample cell at 77 K with the sample being slowly cooled down to 4 K during which the pressure was monitored. The pressure was zero before the temperature reached 25 K, indicating that there would be no bulk hydrogen in the sample. Once the sample reached 4 K, it was allowed to thermally equilibrate for about 3 h before the INS measurements. All INS measurements were performed at around 4 K.

2.3. High pressure experiments

High pressure gas experiments were performed on a fully computer controlled volumetric Sievert's apparatus built at the NCNR [32]. Scientific/research grade H_2 and He gases with purities of 99.9999% were used in all experiments. 107 mg of Pt-SWCNH was loaded into the sample cell in a helium glove box with oxygen and humidity monitors. A valve on the sample cell ensured that the sample was not exposed to air during handling and mounting on the Sievert's apparatus. The sample was evacuated to high vacuum using a turbomolecular pump prior to experiments.

2.4. Density functional theory (DFT) calculation

DFT with B3LYP [33] exchange–correlation potential and the 3-21G atomic basis set was used for the calculations. The geometry of each structure was initially optimized, and then their vibration frequencies were determined by calculating the Hessian matrix [34,35]. The spin due to unpaired hydrogen atoms on the surfaces were taken into account: the number of unpaired electrons was equal to the number of hydrogen atoms on the surface, so the spin was such electrons number divided by two. NWChem package [33–35] was used for all steps of calculations. The neutron scattering spectra from all carbon and spillover hydrogen atoms were calculated and convoluted with the spectral resolution function expected for the experimental configuration of the FANS spectrometer using methodologies within DAVE [36].

3. Results and discussion

Fig. 1(a) shows representative TEM (a,b) and SEM (c) images of carbon nanohorns. SWCNH aggregates have an irregular spherical morphology, and a variety of diameters ranging from 50 nm to 100 nm. A high resolution TEM image (Fig. 1(b)) shows an individual SWCNH aggregate, which is composed of conical tips. The Raman spectrum of SWCNHs (Fig. 2), measured with an excitation of $\lambda = 633$ nm, shows two broad peaks centered at 1317 and 1588 cm^{-1}, which can be assigned to the disorder induced band (D-band) and the G-band associated with the tangential C-C bond stretching vibration in graphitic carbon, respectively. The Raman spectra show that oxidation of SWCNHs results in an increase of the D-band due to introduction of additional defects into SWCNHs during oxidation. The TEM images of oxidized and Pt-decorated SWCNHs (Fig. 3) show relatively uniform distribution of small (2 nm) Pt nanoparticles on the surface of SWCNHs.

During the metal-assisted hydrogen adsorption process, it is believed that hydrogen molecules are dissociated into hydrogen atoms that eventually diffuse to the substrate surfaces. In order to observe the dissociation of hydrogen molecules, we need either a way to monitor the atomic species or the reduction in the amount of molecular hydrogen. INS provides a way to directly estimate the amount of molecular hydrogen in a system. A hydrogen molecule consists of two protons (fermions) requiring the total wavefunction of the molecule to be anti-symmetric [37]. According to the spin state, hydrogen molecules can be separated into two forms: *ortho*-H_2 when the total nuclear spin, S, is 1; and *para*-H_2 when the total nuclear spin is zero. For a free hydrogen molecule, the quantum rotational eigenenergy levels are given by $E = BJ(J + 1)$, where J is the quantum rotation number and $B = 7.35$ meV is the rotational constant. Since the total wavefunction has to be anti-symmetric, J has to be even for *para*-H_2 and J must be odd for *ortho*-H_2. When a neutron interacts with a hydrogen molecule, the nuclear spin may flip causing a *para*-to-*ortho* or *ortho*-to-*para* conversion, and an associated change of the quantum rotational energy. For example, when hydrogen converts from *para*-H_2 to *ortho*-H_2, a scattered neutron will lose 14.7 meV of energy resulting in a peak at 14.7 meV in the INS spectrum. At very low temperature

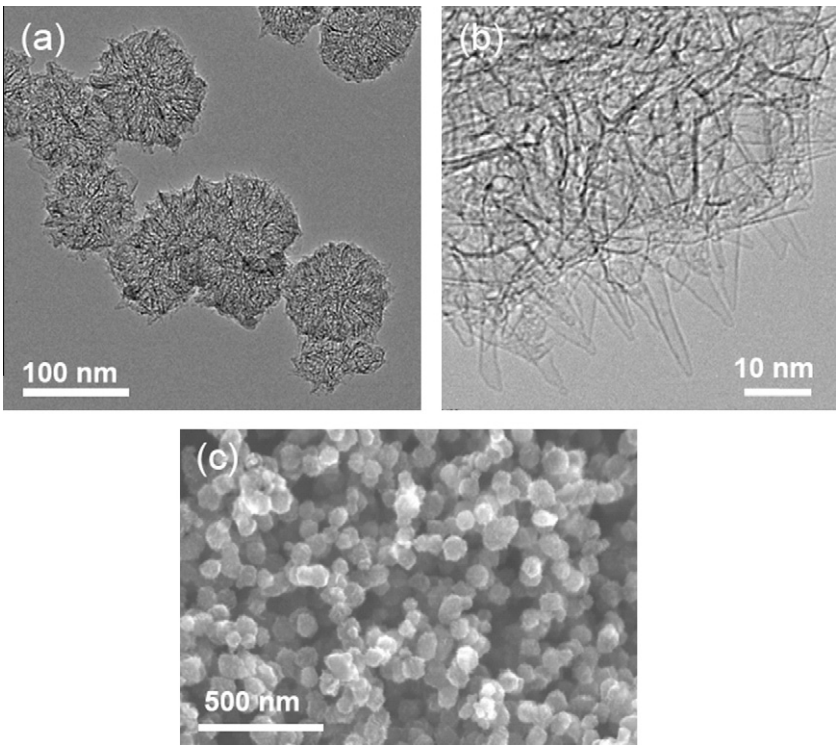

Fig. 1 – (a) TEM, (b) HRTEM, and (c) SEM images of as prepared SWCNH aggregates. Tips of individual nanohorns are shown protruding from an aggregate ball in (b).

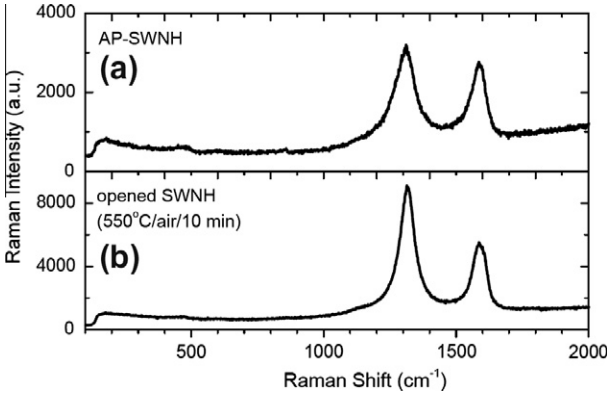

Fig. 2 – Raman spectra of (a) as prepared and (b) oxidized SWCNHs.

(≈4 K), almost all H_2 is converted to *para*-H_2 in our SWCNH samples when the sample temperature is cooled slowly.

Upon adsorption of a hydrogen molecule on a surface, its rotation may be hindered raising the $J = 1$ degeneracy into two or three sublevels. As a result, the rotational peak will become a doublet or triplet depending on the properties of the rotational barrier [38–43]. For hydrogen molecules adsorbed on carbon nanotubes and amorphous carbons, the splitting is usually small with the energy difference between the sublevels less than ≈2 meV [38–44] although this difference can be very large for hydrogen adsorbed at the available metal sites in metal–organic frameworks and zeolites [45–50]. Therefore the rotational peak at ≈14.7 meV in the INS spectra can be used to quantify the existence of molecular hydrogen. By tracing the intensity change of this peak, we can infer if there is a loss of surface-bound hydrogen molecules in our system.

At 77 K, hydrogen molecules are not expected to be dissociated into hydrogen atoms on the nanoscale platinum particles. And it is also more difficult for a hydrogen atom to diffuse on a carbon substrate at such low temperature. Thus, the initial hydrogen dosing (≈1% mass fraction of H_2) was performed at 77 K followed by the first INS measurements at 4 K where all adsorbed hydrogen is due to physisorption. The sample was then warmed to room temperature very slowly and kept at room temperature for 1 day to allow the metal-assisted adsorption process to proceed. The estimated pressure inside the cell is about 0.5 MPa. After waiting at room temperature, the sample was slowly cooled down to 4 K for measurements. We designate this 4 K to 295 K to 4 K process a 'temperature cycle'.

Fig. 4(a) shows a comparison of INS spectra of H_2 adsorbed on Pt-SWCNHs after the subtraction of the un-dosed substrate spectrum. Clearly, the intensity of the rotational peak decreases significantly after the temperature cycle. In order to quantitatively analyze the change of the peak intensity, we fit the peaks with two Gaussian peaks where the full-width at half-maximum (FWHM) of each peak is fixed at the instrumental resolution (1.1 meV) along with a sloping background. The fitted curves are shown in Fig. 4(b) and (c), respectively, and the results listed in Table 1. After the temperature cycle, the total peak area is reduced by ≈17%. Assuming that the relative populations of the hydrogen rotational sublevels are similar between data, the peak area will be linearly proportional to the total amount of H_2 adsorbed in the sample.

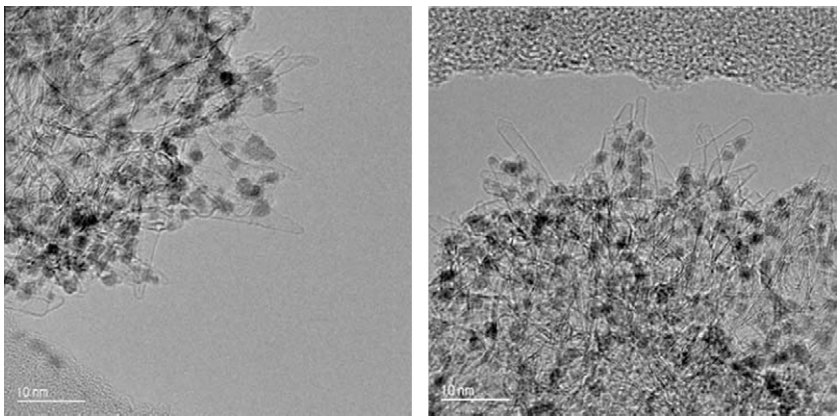

Fig. 3 – TEM images of oxidized, Pt-decorated single wall carbon nanohorns.

In this case, about 0.17% mass fraction of the hydrogen molecules is adsorbed in a different fashion from physisorption at the surface after the temperature cycle. Following the first temperature cycle experiment, we continued to measure the same sample after multiple temperature cycles with the same instrument configurations. The measured INS spectra are identical to the spectrum after the first temperature cycle indicating that there was no hydrogen gas loss due to the leakage of the system during each temperature cycle and that the capacity of metal-assisted hydrogen adsorption is at saturation after one cycle.

Two potential mechanisms could give rise to such a loss of intensity during this metal-assisted adsorption process. The first mechanism is due to hydrogen spillover, where hydrogen molecules are dissociated into hydrogen atoms through interactions with the Pt catalyst at room temperature reducing the number of hydrogen molecules in the system. This loss of hydrogen molecules cannot be explained solely by the formation of Pt hydride. Assuming that the total 'lost' hydrogen is completely adsorbed by the Pt clusters, the atomic ratio between H and Pt atom is about 1.6 in our experiment, much larger than the expected value of ≈0.7 or less [51–53]. As some Pt atoms at the core of individual clusters are less likely to be exposed to hydrogen gas, the ratio between the lost hydrogen and Pt atoms actively interacting with hydrogen is thus expected to be larger than 1.6. Thus, the spillover effect would be a likely scenario. The second mechanism is that hydrogen molecules diffused through the sample at the higher temperature to eventually reach some adsorption sites that could not be accessed at 77 K. The hydrogen molecules' rotation at these new sites would need to be so strongly hindered to render the energy spectrum too broad to be resolved, but cause a decrease in the intensity at ≈14.7 meV. However, given the open structure of the SWCNH, we do not expect significant amount of these special binding sites contributing to the observed molecular hydrogen loss. This will become clearer later when discussing an experiment on a reference sample. Therefore, the observed intensity loss can be most likely attributed to hydrogen loss induced by spillover, and at a minimum, provides an upper limit for the used sample.

We note that previous INS of hydrogen on a Pt/C fuel cell catalyst has directly observed two forms of spillover hydrogen: H at edge sites of a graphite layer, and a weakly bound layer of mobile H atoms [54]. While the vibrational modes were assigned with reference to the INS of a polycyclic aromatic hydrocarbon, the atomic hydrogen was identified from the amplified intensities of the carbon and metal lattice modes due to the 'riding' of the larger scattering cross-section H atoms attached to lattice atoms. Because the details of the vibrational and riding modes for the spillover hydrogen would be expected to be somewhat different depending on the geometry and curvature of the substrate, we have investigated here further theoretically using DFT calculations to predict the INS spectra feature when there are spilled-over hydrogen atoms on carbon surface in the metal-assisted hydrogen adsorption.

We have examined three carbon-cluster structures: graphene, SWNT (6,0) and SWNT (8,0). As shown in Fig. 5 (right), carbon atoms, hydrogen atoms terminating the edges of clusters, and hydrogen atoms on carbon surfaces are shown as gray, white and red balls, respectively. These were chosen to illustrate a more planar geometry compared to a moderate and extremely narrow pore, as may be envisaged for the range of surfaces in a SWCNH cluster. The hydrogen atoms at the edges of the clusters (white) are assigned zero-scattering weight in the calculations of the neutron spectra. Therefore, only the dynamics of the carbon and spillover-hydrogen atoms on carbon surfaces (red) will contribute to the intensity of the simulated INS spectra (Fig. 5, left). In the case of SWNTs, hydrogen atoms on a carbon surface are also separately sited on the inside of the convex surface to provide the extremes of possible binding environments for the spillover hydrogen. The quantity of hydrogen calculated is two on the graphene and SWNT (6,0) surfaces and four on the SWNT (8,0) surfaces. Despite the difference in the geometry of the carbon substrates and the locations of hydrogen atoms on the surfaces, the C–H libration and bending modes for hydrogen atoms on carbon surfaces are predicted to occur at energy transfers between about 50 and 150 meV. The exact details of the predicted spectra are dependent on the geometry of the substrate and locations of hydrogen atoms.

We therefore further attempted to investigate the vibration spectra of our samples using INS and compare them to our DFT calculations to understand the nature of adsorbed hydrogen atoms assisted by Pt metal particles through the temperature cycle. To balance the time-intensive nature of data

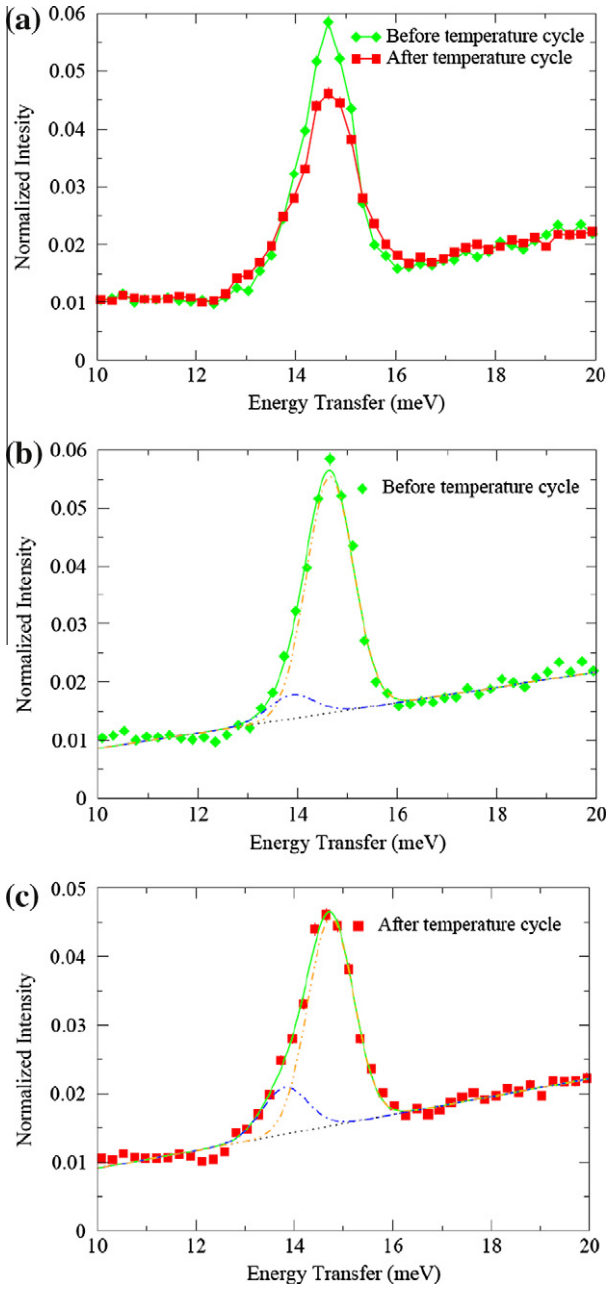

Fig. 4 – (a) Experimental INS data of 1% mass fraction H_2 on Pt-SWCNHs before (solid circles) and after (solid squares) cycling the temperature of the closed system to 295 K. Panels (b) and (c) detail how the peaks are decomposed into a background (dotted line) and two Gaussian peaks (dot-dashed lines) to consistently encapsulate the areas beneath the experimental peaks.

collection, with maximizing information content, we measured the INS spectra from ≈50 to ≈130 meV to cover the energy window most likely to exhibit a discernable difference. The experimental result is the data curve at the bottom of Fig. 5. For this experiment, the sample was preloaded into the sample cell with hydrogen pressure at about 0.5 MPa at room temperature for two weeks. The sample was then evacuated at 77 K for 40 min to remove the majority of molecular hydrogen thereby minimizing the recoil background from molecular hydrogen. The pressure gauge read a steady 3×10^{-3} Pa at the end of evacuation. The sample was again cooled to 4 K for INS measurements. The data are shown in Fig. 6(a). In order to ensure that we can assign the intensity in this region to non-mobile hydrogen at 77 K, the sample was warmed to room temperature and further evacuated for about one hour before cooling the sample back to 4 K for INS measurements. Since metal-assisted hydrogen adsorption is believed to be reversible at room temperature [3,4,6,7], all hydrogen should be pumped out resulting in a measurement of the Pt-SWCNH spectrum only. The difference between the spectra before and after pumping at room temperature is then due to the adsorbed hydrogen at room temperature that cannot be pumped out at 77 K. Even with lengthy counting, there are no prominent peaks in the difference spectrum that only has broad features and displays a slight dip at 90 meV that suggests a broad peak at about 100 meV. The counting statistics are certainly not good enough to claim conclusive observation of C–H modes in this region, though they also do not show any evidence of any intense hydride modes that would be associated with the catalyst as seen in other Pd-carbon systems [2,25,55]. The correlation of broad features and the spectral dip can be interpreted as that rather than having discrete molecular structures from which we calculate vibrational spectra, we have a distribution of adsorption environments over many different positions in a SWCNH cluster. Additionally, the enhanced scattering intensity over this energy range indicates some contributions of the recoil background from hydrogen molecules despite the evacuation of molecular hydrogen at 77 K. Further evidence for this interpretation is indicated by the residual intensity around 14.7 meV as shown in Fig. 6(b). The total area is about 4% of the area of the peak in Fig. 6 (b) or an equivalent of ≈0.04% mass fraction hydrogen. The characteristic rotational peak shape of this residual molecular hydrogen is significantly broader than seen in Fig. 4.

In principle, using this INS method we can also identify the temperature range that metal-assisted hydrogen adsorption can occur. Starting from a fresh sample and loading hydrogen at 77 K, we cycled the temperature to an intermediate temperature, 150 K, instead of room temperature using

Table I – Fitting parameters of the rotational peaks of hydrogen molecules in Pt-SWCNH before and after a single temperature cycle. Standard uncertainties in the fitting results indicate one standard deviation.

	Peak Position (meV)		Peak Area	
	1	2	1	2
Before temperature cycle	13.88 ± 0.13	14.65 ± 0.01	0.0047 ± 0.0013	0.0477 ± 0.0014
After temperature cycle	13.80 ± 0.06	14.74 ± 0.01	0.0080 ± 0.0008	0.0355 ± 0.0009

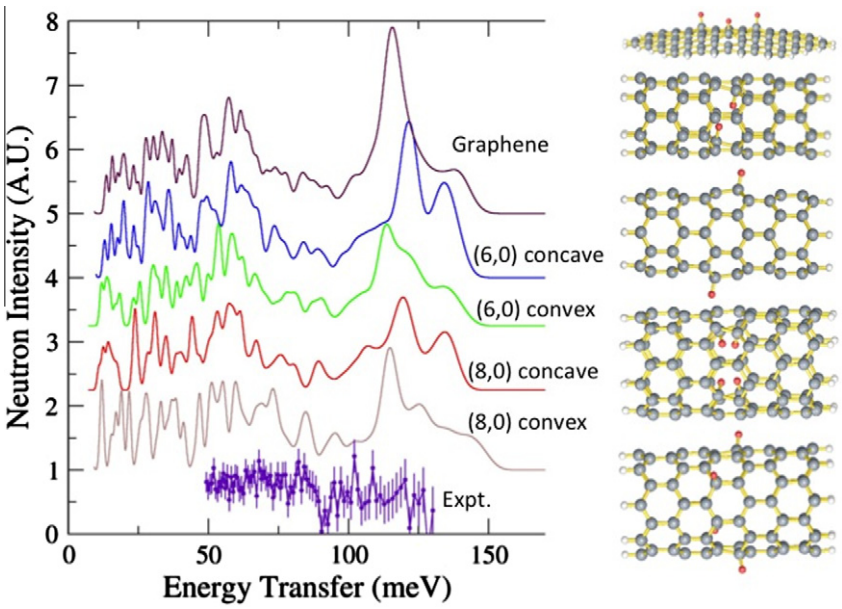

Fig. 5 – The DFT calculation is used to predict the INS spectra due to the librational/vibrational modes of hydrogen atoms. The predicted spectra are shown on the left side of the figure. The right panel shows the structure used in the DFT calculation. Gray, white and red balls indicate carbon atoms, hydrogen atoms at the edge, and hydrogen atoms placed on carbon surfaces, respectively. The simulated INS spectra only contain the contribution from carbon and hydrogen atoms on the carbon surface. Experimental data are shown over the measured energy range as the bottom curve with error bars indicating one standard deviation based on counting statistics. (For interpretation of the references to color in this figure legend, the reader is referred to the web version of this article.)

the same method as above. Comparison of the spectra before and after the temperature cycle is shown in Fig. 7. The two spectra are almost identical indicating that the metal-assisted adsorption process has not occurred below 150 K. To do this exhaustively to pinpoint the exact on-set temperature is beyond the available neutron beamtime we had.

We also performed an identical INS experiment by cycling the temperature to room temperature for a SWCNH sample that was not doped with Pt clusters. As expected, the INS spectra for this SWCNH sample show identical intensity before and after one temperature cycle as shown in Figure S1 in the supporting information. This indicates, as expected, that without Pt clusters, hydrogen molecules could not be dissociated into hydrogen atoms at room temperature resulting in no loss of molecular hydrogen due to metal-assisted adsorption. These results also indicate that all physisorption sites are accessible at 77 K in our SWCNH samples. There is no significant amount of sites that only become accessible at much higher temperature, which further support our previous statement that the observed intensity loss in Fig. 4 for the Pt-SWCNH sample may be most likely due to the spillover effect.

Not only is understanding the temperature onset important, understanding the pressure dependence of metal-assisted hydrogen adsorption is fundamental. In order to address the latter question, we designed a methodology using a volumetric apparatus. An important distinction between the method described here and the dominant literature method to study the metal-assisted hydrogen adsorption at room temperature [56,57] is that we do not rely on the comparison of two different samples. Moreover, this methodology can distinguish between hydrogen adsorption due to spillover and that due to normal physisorption. One important assumption in our implementation of this methodology is that metal-assisted hydrogen adsorption does not occur below 150 K; a fact verified for Pt-SWCNHs using neutron scattering in the preceding paragraphs. The volumetric methodology includes the following steps:

(1) Prepare the sample and load hydrogen gas at 77 K to very high pressure (in our experiment, the pressure is about 5 MPa) and record the equilibrium pressure, P_0. The system is now isolated so that the total amount of hydrogen in the system is fixed.
(2) Warm the sample to a known temperature and wait a time t_w to allow metal-assisted hydrogen adsorption to occur.
(3) Cool the sample back to 77 K again and record the equilibrium pressure, P_1.
(4) From the difference of P_0 and P_1, we can estimate the amount of gas adsorbed due to the metal-assisted hydrogen adsorption, which is potentially due to hydrogen spillover.

If $P_0 = P_1$, there is no metal-assisted adsorption. If $P_0 > P_1$, metal-assisted hydrogen adsorption has occurred during the temperature cycle which could be potentially due to spillover. The pressure should return to the same value if physisorption was the sole hydrogen adsorption mechanism present (in the absence of additional porosity being available through structural or other changes in the material). We have applied this methodology to quantitatively estimate the amount of extra hydrogen adsorbed by cycling the sample temperature.

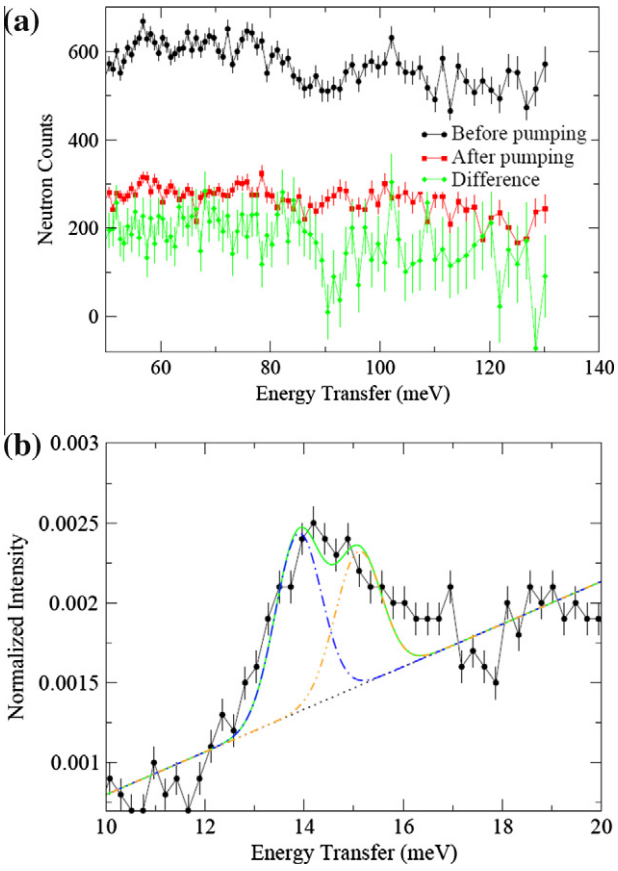

Fig. 6 – (a) INS data (at 4 K) of residual hydrogen on Pt-SWCNHs after evacuating the system at 77 K (black circles) compared to that after evacuating the system at 295 K (red squares). The difference is the residual hydrogen scattering that is not mobile at 77 K (green diamonds). (b) Residual hydrogen that is not evacuated at 77 K also gives rise to a molecular *para–ortho* scattering intensity that is approximately 0.04% mass fraction loading equivalent. Error bars indicate one standard deviation based on counting statistics. (For interpretation of the references to color in this figure legend, the reader is referred to the web version of this article.)

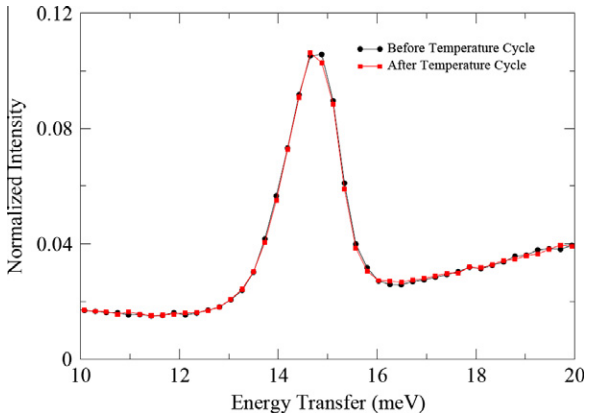

Fig. 7 – Experimental INS data of 1% mass fraction H_2 on Pt-SWCNHs before (black circles) and after (red squares) cycling the temperature of the closed system to 150 K. All measurements were taken at 4 K.

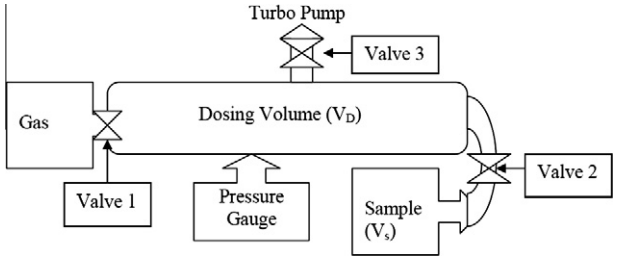

Fig. 8 – Schematic of the homemade Sievert's apparatus used in our high-pressure gas experiments. Valve 1 controls the dosing of hydrogen gas to the dosing volume, V_D. There is a gas line connecting the dosing volume to the sample via Valve 2. The dosing volume and gas line up to Valve 2 are maintained at room temperature. The sample volume, V_S, and the gas loading line after valve 2 are cooled to the sample temperature, T_S, which is controlled using a cryostat.

Fig. 8 shows a schematic of the volumetric Sievert's apparatus [32] used in our high-pressure gas experiments. The dosing volume (V_D) is connected via Valve 2 to the sample. While the gas and dosing volume remain at room temperature (T_D), the sample and the gas loading line after Valve 2 are at the sample temperature, T_S, which is controlled using a cryostat. Since the laboratory temperature can fluctuate as a function of time causing a pressure fluctuation in the dosing volume, we recorded the temperature of the dosing volume to correct for this effect. There are four temperature sensors around the dosing volume and the average temperature is used to compute the temperature of the dosing volume, T_D. While T_D may vary by about 2 K, T_S is very stable with a negligible fluctuation on the order of 0.1 K. Since $V_s << V_D$, the recorded pressures of both P_0 and P_1 are much more sensitive to T_D than T_S.

After loading the sample into the apparatus, ≈5 MPa of He gas was used to test for leakage. The system was deemed leak-free since the pressure fluctuation over 17 h at room temperature was less than ≈7 kPa after correction for temperature (T_D) effect. After removing the He gas at room temperature, the experiment proceeded by cooling the sample to 77 K (T_S = 77 K) and then admitting ≈4.8 MPa H_2 gas into the dosing volume and sample cell followed by monitoring the pressure (P_0) fluctuation as a function of T_D over a period of 19 h (Fig. 9). Due to the fluctuation of T_D, P_0 fluctuated ≈20 kPa. Although this pressure change seems small compared to the total pressure, it will affect the results significantly if it is not taken into account. In fact, for the sample mass and volumes used here, a difference of 50 kPa between the cycle pressures P_0 and P_1 would indicate an additional ≈1% mass fraction hydrogen.

For the second step the sample was warmed to 300 K where it was maintained for about 17 h before step 3, where it was cooled back to 77 K again. After this 1st temperature cycle, the equilibrium pressure, P_1, was recorded again at 77 K (over a period of 1 h) as a function of T_D, as summarized in Fig. 8. In this case, T_D fluctuated much less than previously, reflecting the variability in the laboratory ambient temperature and

the reduced monitoring period. For a particular value of T_D, P_1 is smaller than P_0 indicating that extra hydrogen is adsorbed due to the first temperature cycle. We performed the 2nd temperature cycle, this time waiting overnight at room temperature before cooling back to 77 K, and monitoring the equilibrium pressure, P_2, at 77 K.

Based on the pressure difference, we can estimate the adsorbed hydrogen due to metal-assisted adsorption. In order to correct the effect of the fluctuating T_D, we need to first estimate how a nominal pressure (P) varies as a function of T_D. The total gas volume can be separated into two parts: V_D and V_S. Since the sample temperature is very stable, the amount of gas in V_S is not sensitive to T_D. Denoting N_D and N_S as the moles of H_2 gas in V_D and V_S, we can calculate the total amount of hydrogen molecules in gas phase, N, with the following equations:

$$\begin{aligned} N_D &= \tfrac{P_D V_D}{R T_D} \\ N_S &= \tfrac{P_S V_S}{R T_S} \\ P_D &= P_S = P \\ N &= N_D + N_S \end{aligned} \qquad (1)$$

where R is the ideal gas constant, P_D and P_S are the pressures in V_D and V_S. From the above equations, we obtain:

$$P = \frac{N R T_D}{V_D} \frac{1}{(1 + \frac{V_S}{V_D}\frac{T_D}{T_S})} \qquad (2)$$

Since P, V_S, V_D, T_S, and T_D are known, we obtain N, the amount of hydrogen in the gas phase, by fitting the data points in Fig. 9. For this Sievert's apparatus, V_D = 22.6 ml and V_S = 0.8 ml. Although there is a temperature gradient from Valve 2 along the gas line to the sample cell, the volume in the gas line is small enough that this effect can be ignored.

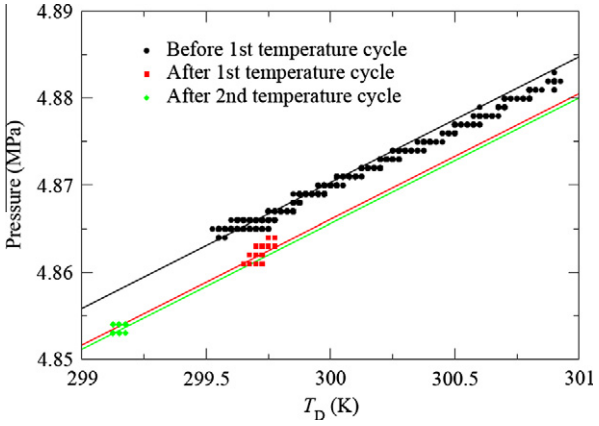

Fig. 9 – Fluctuations in system pressure reading as a function of the dosing volume temperature (T_D) over a period of time. Initial dosing pressures at 77 K, P_0, (black circles) were recorded over 19 h. The sample was then warmed to room temperature for 17 h before being cooled back to 77 K where P_1 is monitored (red squares). A second temperature cycle was followed by monitoring the pressure, P_2, at 77 K (green diamonds). Lines are fits to the data using equation 2 as described in the text. (For interpretation of the references to color in this figure legend, the reader is referred to the web version of this article.)

Fitting P_0 as a function of T_D, we obtain the amount of H_2 in the gas phase, N_0. Similarly by fitting P_1 and P_2, the amount of gaseous H_2, N_1 and N_2, can be calculated. Comparing the difference between N_0 and N_1 or N_2, we know the amount of molecular hydrogen adsorbed upon cycling the temperature. The extra adsorbed hydrogen after the first temperature cycle is estimated to be about 0.08% mass fraction. The second temperature cycle only introduces an extra ≈0.01% mass fraction hydrogen adsorption indicating that the adsorption due to the temperature cycling is almost saturated after our first temperature cycle. If we assume that the amount of physisorbed hydrogen molecules is the same before and after the 1st temperature cycle, these results are consistent with the results we obtain using INS where the upper limit of hydrogen adsorption due to the metal-assisted process is around 0.17% mass fraction at a lower pressure. The small difference of the results between this method and the INS method is expected since the samples were treated separately between the two experiments.

Although we had applied about 5 MPa of hydrogen gas in our experiments, the pressure can be chosen at any value so that the amount of hydrogen adsorbed through the temperature cycle can be measured as a function of the total applied pressure. Because the current batch of samples does not have a large amount of hydrogen due to metal-assisted adsorption at high pressure, we did not proceed further to measure our samples at different pressures.

It should be noted that our Pt-SWCNH samples can adsorb up to more than 2.0% mass fraction hydrogen molecules due to physisorption at 77 K. The additional hydrogen adsorption after the temperature cycle is very small contribution to the hydrogen adsorption at 77 K. The hydrogen adsorption capability for the Pt-SWCNH samples varies from about 0.3% mass fraction to 0.8% mass fraction at room temperature. The variation of the measured results again demonstrates the importance to identify the hydrogen adsorption due to the metal-assisted adsorption using one sample only. The comparison of a reference sample would not be accurate to estimate the enhanced adsorption due to the metal-assisted effect. Through our careful measurements here using both INS and high pressure gas adsorption techniques, we can conclude that the overall contribution for hydrogen storage related with the presence of Pt catalytic metal particles is about 0.1% mass fraction for the used samples. As the formation of possible Pt hydride alone could not explain the loss of hydrogen molecules through the temperature cycle, it is hence reasonable to conclude that the hydrogen molecules are dissociated into hydrogen atoms and diffuse to the carbon surface and strongly bound there. Given that total hydrogen adsorption at room temperature up to about 5 MPa ranges from 0.3% to 0.5% mass fraction in both metal-decorated and undecorated samples measured with our Sievert's apparatus, 0.1% mass fraction hydrogen adsorption is already very significant. However, we did not observe a linear increase of adsorbed hydrogen molecule due to metal-assisted adsorption when the gas pressure increases from about 0.5 to about 5 MPa as compared with some early reports [3–5] although the total hydrogen adsorption still increases linearly with the pressure. As pointed out in Ref. [14], there are many factors, such as metal concentration, size of catalytic metal particles,

and sample pretreatment that could affect the final results of metal-assisted hydrogen storage. The detailed reasons for the difference of the pressure dependence of metal-assisted hydrogen adsorption need further investigation.

The proposed two methodologies have different advantages, limitations, and assumptions. The INS experiment can directly measure the concentration change of hydrogen molecules. But, when cycling the temperature, the relative population of para-H_2 and ortho-H_2 changes also. Therefore, the temperature of a sample must be cooled slowly so that the majority of hydrogen molecules can be converted back to para-H_2 at about 4 K. If the sample temperature is not cooled sufficiently slowly, some ortho-H_2 might become strongly bound to particular adsorption sites and not converted to para-H_2. The unconverted ortho-H_2 will thus affect the estimation of the amount of hydrogen molecules before and after the temperature cycling. A limitation of this technique is that the initial amount of hydrogen loaded at low temperature, must, at most, only be adsorbed on the surface of the sample and not give rise to condensed bulk hydrogen; as such the maximum pressure reachable in a given heating cycle is determined by the volume of the enclosed system and surface area of the material. Finally, this type of INS experiment requires a significant amount of beam time and is only available at specialized neutron scattering facilities.

In contrast to the INS experiment, a high-pressure Sievert's apparatus is much more readily available for most research groups and can measure pressure changes over a very large pressure range. If the additional adsorbed hydrogen atoms due to metal-assisted adsorption process do not block the adsorption sites of hydrogen molecules attempting to physisorb upon cooling down again to 77 K, then the proposed method using Sievert's-type apparatus to quantitatively measure the metal-assisted hydrogen adsorption is very accurate. However, if the adsorbed hydrogen atoms fill pores or sites previously used for physisorption, then the Sievert's method will correspondingly underestimate the amount of adsorbed spillover hydrogen atoms. To the best of our knowledge, no experimental investigation has determined how adsorbed hydrogen atoms (e.g. from spillover) affect physisorption of hydrogen molecules.

4. Conclusions

Inelastic neutron scattering (INS) and Sievert's method measurements have been combined with temperature-cycling to assess the role of temperature-activated, metal-assisted hydrogen storage in single samples. These methods do not rely upon comparative adsorption measurements between metal-decorated and undecorated samples, and enable the unambiguous detection of smaller adsorbed quantities of metal-assisted hydrogen adsorption. These techniques were tailored to investigate hydrogen storage resulting from temperature-activated processes such as spillover, and were applied here for Pt-decorated single-wall carbon nanohorns (Pt-SWCNHs). The INS technique measures quantum rotational transitions of molecular hydrogen or vibration modes of C–H bonds to more accurately and selectively quantify both molecular hydrogen or bonded atomic hydrogen in single samples.

INS measurements on single samples of SWCNHs decorated with 2–3 nm Pt nanoparticles showed a 0.17% mass fraction loss of molecular hydrogen after the sample was loaded at 77 K then cycled to room temperature (at pressure of about 0.5 MPa) and back to 4 K. However no loss in hydrogen was observed when it was cycled only up to 150 K. Control samples using undecorated SWCNHs did not display any loss of molecular hydrogen measured at 4 K after cycling to room temperature. Similar measurements involving temperature cycling of Pt-decorated SWCNHs charged with 5 MPa of hydrogen at 77 K using a Sievert's apparatus also indicated a measurable quantity (≈0.08% mass fraction) of metal-assisted hydrogen adsorption caused by cycling samples to room temperature.

When one considers that different samples (both metal-decorated and undecorated) exhibited variations in room-temperature excess hydrogen storage ranging between 0.3–0.5% mass fraction at 5 MPa in the current study, the ability to unambiguously detect 0.1–0.2% mass fraction changes in single samples and assign these to metal-assisted, temperature-activated processes is highly significant. Although it appears that the metal-assisted storage in the current experiments does not scale with applied pressure (linear scaling has been observed in spillover [3,5]), the 0.17% mass fraction excess measured at 0.5 MPa in the Pt-SWCNHs is clearly related to temperature-activated, metal-assisted storage, is too large for physisorption alone, and cannot be explained solely by platinum hydride formation.

These measurements present clear evidence for additional excess storage measured at low temperatures induced by metal-assisted activated processes at room temperature, which to our knowledge has never been demonstrated before. This technique therefore is most useful to investigate temperature-activated processes which might involve additional binding sites, for example spillover where C–H bonds might be expected. DFT calculations were performed to predict signature INS spectra for C–H libration and bending modes for various conformations of carbon with hydrogen attached in different configurations. However, measured INS spectra revealed a near-continuum spectrum different from the predicted sharp peaks by our DFT calculations, indicating a lack of one preferred binding site if chemically-bonded H occurred in these samples. This is not unexpected due to the great variety of curvatures inherent in the different adsorption sites on SWCNHs. While currently we cannot identify the exact nature of the binding of the additional hydrogen in these experiments, our measurements do confirm the loss of molecular hydrogen and significant metal-assisted hydrogen storage on Pt-SWCNHs that is activated at $T > 150$ K which is consistent with spillover.

Acknowledgements

Work at NIST was partially supported by the Office of Energy Efficiency and Renewable Energy (EERE) through the Hydrogen Sorption Center of Excellence. Synthesis science on carbon nanostructure growth was funded by the Division of Materials Sciences and Engineering, Office of Basic Energy Sciences at DOE. Characterization of SWCNHs was funded by EERE Center

of Excellence on Hydrogen Sorption Center of Excellence and independent research at the Center for Nanophase Materials Sciences and SHaRE User Facility, Division of Scientific User Facilities, DOE-BES. Oak Ridge National Laboratory is operated under the management of UT-Battelle, L.L.C. for the US Department of Energy under Contract No. DE-AC05-00OR22725.

Appendix A. Supplementary data

Supplementary data associated with this article can be found, in the online version, at http://dx.doi.org/10.1016/j.carbon.2012.06.028.

REFERENCES

[1] Schlapbach L, Zuttel A. Hydrogen-storage materials for mobile applications. Nature 2001;414(6861):353–8.
[2] Lueking A, Yang RT. Hydrogen spillover from a metal oxide catalyst onto carbon nanotubes – Implications for hydrogen storage. J Catal 2002;206(1):165–8.
[3] Li YW, Yang RT. Hydrogen storage in metal-organic frameworks by bridged hydrogen spillover. J Am Chem Soc 2006;128(25):8136–7.
[4] Li YW, Yang RT. Significantly enhanced hydrogen storage in metal-organic frameworks via spillover. J Am Chem Soc 2006;128(3):726–7.
[5] Li YW, Yang RT. Hydrogen storage on platinum nanoparticles doped on superactivated carbon. J Phys Chem C 2007;111:11086–94.
[6] Li YW, Yang FH, Yang RT. Kinetics and mechanistic model for hydrogen spillover on bridged metal-organic frameworks. J Phys Chem C 2007;111(8):3405–11.
[7] Lachawiec AJ, DiRaimondo TR, Yang RT. A robust volumetric apparatus and method for measuring high pressure hydrogen storage properties of nanostructured materials. Rev Sci Instrum 2008;79(6):12.
[8] Luzan SM, Talyzin AV. Hydrogen adsorption in Pt catalyst/MOF-5 materials. Microporous Mesoporous Mat 2010;135(1–3):201–5.
[9] Stadie NP, Purewal JJ, Ahn CC, Fultz B. Measurements of hydrogen spillover in platinum doped superactivated carbon. Langmuir 2010;26(19):15481–5.
[10] Kunowsky M, Marco-Lozar JP, Cazorla-Amoros D, Linares-Solano A. Scale-up activation of carbon fibres for hydrogen storage. Int J Hydrog Energy 2010;35(6):2393–402.
[11] Campesi R, Cuevas F, Latroche M, Hirscher M. Hydrogen spillover measurements of unbridged and bridged metal-organic frameworks-revisited. Phys Chem Chem Phys 2010;12(35):10457–9.
[12] Bhatia SK, Myers AL. Optimum conditions for adsorptive storage. Langmuir 2006;22(4):1688–700.
[13] Schmitz B, Muller U, Trukhan N, Schubert M, Ferey G, Hirscher M. Heat of adsorption for hydrogen in microporous high-surface-area materials. Chem Phys Chem 2008;9(15):2181–4.
[14] Stuckert NR, Wang LF, Yang RT. Characteristics of hydrogen storage by spillover on Pt-doped carbon and catalyst-bridged metal organic framework. Langmuir 2010;26(14):11963–71.
[15] Tsao CS, Tzeng YR, Yu MS, Wang CY, Tseng HH, Chung TY, et al. Effect of catalyst size on hydrogen storage capacity of pt-impregnated active carbon via spillover. J Phys Chem Lett 2010;1(7):1060–3.
[16] Psofogiannakis GM, Steriotis TA, Bourlinos AB, Kouvelos EP, Charalambopoulou GC, Stubos AK, et al. Enhanced hydrogen storage by spillover on metal-doped carbon foam: an experimental and computational study. Nanoscale 2011;3(3):933–6.
[17] Wang LF, Yang FH, Yang RT, Miller MA. Effect of surface oxygen groups in carbons on hydrogen storage by spillover. Ind Eng Chem Res 2009;48(6):2920–6.
[18] Li QX, Lueking AD. Effect of surface oxygen groups and water on hydrogen spillover in Pt-doped activated carbon. J Phys Chem C 2011;115(10):4273–82.
[19] Wang Z, Yang FH, Yang RT. Enhanced hydrogen spillover on carbon surfaces modified by oxygen plasma. J Phys Chem C 2010;114(3):1601–9.
[20] Sermon PA, Bond GC. Hydrogen spillover. Catal Rev-Sci Eng 1973;8(2):211–39.
[21] Taylor H. Surface Catalysis. Annu Rev Phys Chem 1961;12:127–50.
[22] Khoobiar S. Particle to particle migration of hydrogen atoms on platinum-alumina catalysts from particle to neighboring particles. J Phys Chem. 1964;68(2):411–2.
[23] Robell AJ, Ballou EV, Boudart M. Surface diffusion of hydrogen on carbon. J Phys Chem 1964;68(10):2748–53.
[24] Conner WC, Falconer JL. Spillover in heterogeneous catalysis. Chem Rev 1995;95(3):759–88.
[25] Yang FH, Lachawiec AJ, Yang RT. Adsorption of spillover hydrogen atoms on single-wall carbon nanotubes. J Phys Chem B 2006;110(12):6236–44.
[26] Yang RT, Wang YH. Catalyzed hydrogen spillover for hydrogen storage. J Am Chem Soc 2009;131(12):4224–6.
[27] Tsao CS, Liu Y, Chuang HY, Tseng HH, Chen TY, Chen CH, et al. Hydrogen spillover effect of Pt-doped activated carbon studied by inelastic neutron scattering. J Phys Chem Lett 2011;2(18):2322–5.
[28] Cheng MD, Lee DW, Zhao B, Hu H, Styers-Barnett DJ, Puretzky AA, et al. Formation studies and controlled production of carbon nanohorns using continuous in situ characterization techniques. Nanotechnology 2007;18(18):8.
[29] Puretzky AA, Styers-Barnett DJ, Rouleau CM, Hu H, Zhao B, Ivanov IN, et al. Cumulative and continuous laser vaporization synthesis of single wall carbon nanotubes and nanohorns. Appl Phys A-Mater Sci Process 2008;93(4):849–55.
[30] Udovic TJ, Brown CM, Leao JB, Brand PC, Jiggetts RD, Zeitoun R, et al. The design of a bismuth-based auxiliary filter for the removal of spurious background scattering associated with filter-analyzer neutron spectrometers. Nucl Instrum Methods Phys Res Sect A-Accel Spectrom Dect Assoc Equip 2008;588(3):406–13.
[31] Copley JRD, Neumann DA, Kamitakahara WA. Energy distributions of neutrons scattered from solid C-60 by the beryllium detector method. Can J Phys 1995;73(11–12):763–71.
[32] Zhou W, Wu H, Hartman MR, Yildirim T. Hydrogen and methane adsorption in metal-organic frameworks: A high-pressure volumetric study. J Phys Chem C 2007;111(44):16131–7.
[33] Becke AD. Density-functional thermochemistry.3. The role of exact exchange. J Chem Phys 1993;98(7):5648–52.
[34] Straatsma TP, Aprà E, Windus TL, Bylaska EJ, de Jong W, Hirata S, et al. NWChem, A Computational Chemistry Package for Parallel Computers, Version 4.6 (2004), Pacific Northwest National Laboratory, Richland, Washington 99352–0999, USA.
[35] Kendall RA, Aprà E, Bernholdt DE, Bylaska EJ, Dupuis M, Fann GI, et al. High performance computational chemistry: An overview of NW Chem a distributed parallel application. Computer Phys Comm 2000;128:260–83.
[36] Azuah RT, Kneller LR, Qiu YM, Tregenna-Piggott PLW, Brown CM, Copley JRD, et al. Dave: a comprehensive software suite

for the reduction, visualization, and analysis of low energy neutron spectroscopic data. J Res Natl Inst Stand Technol 2009;114(6):341–58.
[37] Silvera IF. The solid molecular hydrogens in the condensed phase – fundamentals and static properties. Rev Mod Phys 1980;52(2):393–452.
[38] FitzGerald SA, Yildirim T, Santodonato LJ, Neumann DA, Copley JRD, Rush JJ, et al. Quantum dynamics of interstitial H-2 in solid C-60. Phys Rev B 1999;60(9):6439–51.
[39] Brown CM, Yildirim T, Neumann DA, Heben MJ, Gennett T, Dillon AC, et al. Quantum rotation of hydrogen in single-wall carbon nanotubes. Chem Phys Lett 2000;329(3–4):311–6.
[40] Liu Y, Brown CM, Blackburn JL, Neumann DA, Gennett T, Simpson L, et al. Inelastic neutron scattering of H-2 adsorbed on boron substituted single walled carbon nanotubes. J Alloys Compd 2007;446–447:368–72.
[41] Yildirim T, Harris AB. Rotational and vibrational dynamics of interstitial molecular hydrogen. Phys Rev B 2002;66(21):20.
[42] Schimmel HG, Kearley GJ, Mulder FM. Resolving rotational spectra of hydrogen adsorbed on a single-walled carbon nanotube substrate. Chem Phys Chem 2004;5(7):1053–5.
[43] Georgiev PA, Giannasi A, Ross DK, Zoppi M, Sauvajol JL, Stride J. Experimental Q-dependence of the rotational $J = 0$-to-1 transition of molecular hydrogen adsorbed in single-wall carbon nanotube bundles. Chem Phys 2006;328(1–3):318–23.
[44] Georgiev PA, Ross DK, De Monte A, Montaretto-Marullo U, Edwards RAH, Ramirez-Cuesta AJ, et al. In situ inelastic neutron scattering studies of the rotational and translational dynamics of molecular hydrogen adsorbed in single-wall carbon nanotubes (SWNTs). Carbon 2005;43(5):895–906.
[45] Brown CM, Liu Y, Yildirim T, Peterson VK, Kepert CJ. Hydrogen adsorption in HKUST-1: a combined inelastic neutron scattering and first-principles study. Nanotechnology 2009;20(20):11.
[46] Liu Y, Brown CM, Neumann DA, Peterson VK, Kepert CJ. Inelastic neutron scattering of H-2 adsorbed in HKUST-1. J Alloys Compd 2007;446–447:385–8.
[47] Liu Y, Kabbour H, Brown CM, Neumann DA, Ahn CC. Increasing the density of adsorbed hydrogen with coordinatively unsaturated metal centers in metal-organic frameworks. Langmuir 2008;24(9):4772–7.
[48] Dietzel PDC, Georgiev PA, Eckert J, Blom R, Strassle T, Unruh T. Interaction of hydrogen with accessible metal sites in the metal-organic frameworks M-2(dhtp) (CPO-27-M; M=Ni, Co., Mg).. Chem Commun. 2010;46(27):4962–4.
[49] Eckert J, Nicol JM, Howard J, Trouw FR. Adsorption of Hydrogen in Ca-Exchanged Na-A Zeolites Probed by Inelastic Neutron Scattering Spectroscopy. J Phys Chem 1996;100:10646–51.
[50] Nicol JM, Eckert J, Howard J. Dynamics of molecular hydrogen adsorbed in CoNa-A zeolite. J Phys Chem 1988;92:7117–21.
[51] Oudenhuijzen MK, Bitter JH, Koningsberger DC. The nature of the Pt-H bonding for strongly and weakly bonded hydrogen on platinum. A XAFS spectroscopy study of the Pt-H antibonding shaperesonance and Pt-H EXAFS. J Phys Chem B 2001;105(20):4616–22.
[52] Wanke SE, Lotochinski BK, Sidwell HC. Hydrogen adsorption measurements by the dynamic pulse method. Can J Chem Eng 1981;59(3):357–61.
[53] Flynn PC, Wanke SE. Effect of pretreatment and adsorption conditions on gas adsorption by supported metal-catalysts. Can J Chem Eng 1975;53(6):636–40.
[54] Mitchell PCH, Ramirez-Cuesta AJ, Parker SF, Tomkinson J, Thompsett D. Hydrogen spillover on carbon-supported metal catalysts studied by inelastic neutron scattering. Surface vibrational states and hydrogen riding modes. J Phys Chem B 2003;107(28):6838–45.
[55] Contescu CI, Brown CM, Liu Y, Bhat VV, Gallego NC. Detection of hydrogen spillover in palladium-modified activated carbon fibers during hydrogen adsorption. J Phys Chem C 2009;113(14):5886–90.
[56] Mavrandonakis A, Klopper W. Kinetics and mechanistic model for hydrogen spillover on bridged metal–organic frameworks. J Phys Chem C 2008;112(8):3152–4.
[57] Li YW, Yang FH, Yang RT. Reply to "Comment on 'Kinetics and Mechanistic Model for Hydrogen Spillover on Bridged Metal–Organic Frameworks'". J Phys Chem C 2008;112(8):3155–6.